

# X-rays from the episodic dust maker WR 137

Svetozar A. Zhekov<sup>\*</sup>

*Space Research and Technology Institute, Akad. G. Bonchev str., bl.1, Sofia 1113, Bulgaria*

## ABSTRACT

We present an analysis of the *XMM-Newton* observation of the episodic dust maker WR 137. Global spectral fits show that its X-ray spectrum is well matched by a two-temperature optically-thin plasma emission ( $kT_1 \sim 0.4$  keV and  $kT_2 \sim 2.2$  keV). If we adopt the colliding stellar wind (CSW) picture for this wide WR+O binary, the theoretical CSW spectra match well the shape of the observed X-ray spectrum of WR 137 but they overestimate the observed flux (emission measure) by about two orders of magnitude. To reconcile the model predictions with observations, the mass loss of WR 137 must be reduced considerably (by about an order of magnitude) with respect to its currently accepted value. In all the spectral fits, the derived X-ray absorption is consistent with the optical extinction to WR 137.

**Key words:** shock waves — stars: individual: WR 137 — stars: Wolf-Rayet — X-rays: stars.

## 1 INTRODUCTION

Wolf-Rayet (WR) stars are massive stars that are descendants from the massive O-type stars. WR stars have powerful winds and are losing mass at high rates ( $\dot{M} \sim 10^{-5} M_{\odot} \text{ yr}^{-1}$ ;  $V_{\text{wind}} = 1000 - 3000 \text{ km s}^{-1}$ ). There are three spectral sequences depending on the abundance of light metals: nitrogen-rich (WN), carbon-rich (WC) and oxygen-rich (WO) Wolf-Rayet stars. The observed binary fraction in the WR stars in the Galaxy is relatively high and about 40% of them are members of WR+O systems (van der Hucht 2001).

There is a class of WRs, so called episodic dust makers (EDM), which show recurrent infrared bursts that fade away with time (e.g. Williams 1995; 2008 and the references therein). Seven WC stars are known EDMs. These are WR 19, WR 48a, WR 70, WR 98a, WR 125, WR 137 and WR 140. All of these objects possess variable NIR/IR emission characterized by at least one ‘burst’, that is a rapid rise of their emission that faded away in a period of time (a few months and even years). For some of these objects, it is certain that the WC star is a member of a binary system with the same period of their recurrent IR emission: WR 140 (Williams et al. 1990; Williams 2011 and the references therein), WR 137 (Lefèvre et al. 2005). For others, binarity is suspected based on presence of absorption lines in their optical spectra that are typical for massive O stars or it is suggested by the dilution of their spectral lines.

It is believed that colliding stellar winds (CSW) in massive WR binaries play a key role for the physics of EDMs and more specifically for the origin of their infrared, radio

and X-ray emission. Apart from their periodic IR emission, the EDMs should possess strong X-ray emission and they should be non-thermal radio sources. These basic characteristics are best illustrated by the prototype EDM object, the WR+O binary WR 140. They are reasonably well explained as a result from CSWs in a wide binary system with highly elliptical orbit (Williams et al. 1990).

We recall that a very basic feature of CSWs is their strong X-ray emission that originates from the interaction region of the winds of the massive binary components (Prilutskii & Usov 1976; Cherepashchuk 1976). This likely explains the fact that came out from the first systematic survey of WRs: the WR+O binaries are the brightest X-ray sources amongst WR stars (Pollock 1987). In the framework of the CSW picture, one can thus expect that all the episodic dust makers should possess an enhanced X-ray emission.

The X-ray emission from two episodic dust makers is studied in considerable detail. The prototype EDM, WR 140, has been detected with almost all the X-ray observatories (e.g., Williams et al. 1990; Zhekov & Skinner 2000; Pollock et al. 2005; Williams 2011). It has variable X-ray emission, variable X-ray absorption, its X-ray plasma is hot ( $kT \geq 3$  keV). The analysis of recent *XMM-Newton* and *Chandra* data on WR 48a showed that this is the most X-ray luminous WR star in the Galaxy detected so far, after the black hole candidate Cyg X-3 and its dominant temperature component is  $kT \approx 3$  keV (Zhekov et al. 2011; 2014). The luminous X-ray emission and the high plasma temperature can be considered as a solid sign for presence of CSWs in these objects. Similar findings for other EDMs are thus needed to check the validity of the CSW paradigm for this class of objects.

<sup>\*</sup> E-mail: szhekov@space.bas.bg

In this paper, we report results from the *XMM-Newton* observation of WR 137, the third object amongst the episodic dust makers with an acceptably good quality of its X-ray spectra. The paper is organized as follows. We give some basic information about WR 137 in Section 2. In Section 3, we review the *XMM-Newton* observation. In Section 4, we present results from analysis of the X-ray properties of WR 137. In Section 5, we discuss our results, and we present our conclusions in Section 6.

## 2 THE WOLF-RAYET STAR WR 137

WR 137 (HD 192641) is one of the seven WR stars that originally formed the group of episodic dust makers (Williams 1995). It is a spectroscopic binary (WC7pd+O9) with an orbital period of  $4765 \pm 50$  days at a distance of 2.38 kpc (van der Hucht 2001). The binary period was derived from analysis of the infrared variability, that is from the consecutive dust-formation episodes (Williams et al. 2001). It was later confirmed by spectroscopic studies in the optical domain:  $4766 \pm 66$  days (Lefèvre et al. 2005). The optical extinction toward WR 137 is  $A_v = 1.97$  mag (van der Hucht 2001;  $A_v = 1.11$  A<sub>V</sub>) implying a foreground column density of  $N_H = (2.94 - 3.94) \times 10^{21} \text{ cm}^{-2}$ . The range corresponds to the conversion that is used:  $N_H = (1.6 - 1.7) \times 10^{21} \text{ A}_V \text{ cm}^{-2}$  (Vuong et al. 2003, Getman et al. 2005); and  $N_H = 2.22 \times 10^{21} \text{ A}_V \text{ cm}^{-2}$  (Gorenstein 1975). We adopt the stellar wind parameters (velocity and mass loss) of  $V_{\text{wind}} = 1885 \text{ km s}^{-1}$  and  $\dot{M} = 3 \times 10^{-5} M_\odot \text{ yr}^{-1}$  (Nugis et al. 1998).

In radio, no in detail studies are carried out so far. WR 137 was classified as a thermal radio source by Abbott et al. (1986) and it was also listed as a non-thermal radio source in Dougherty & Williams (2000) but that classification was based only on a private communication.

In X-rays, a marginal detection was reported from the *Einstein* survey of Wolf-Rayet stars,  $L_X = 1.6 \pm 1.1 \times 10^{32} \text{ ergs s}^{-1}$  (Pollock 1987), and also from the *ROSAT* survey of Wolf-Rayet stars,  $L_X = 0.61 \pm 0.10 \times 10^{32} \text{ ergs s}^{-1}$  (Pollock et al. 1995). Both data sets had poor photon statistics ( $\leq 50$  source counts).

## 3 OBSERVATIONS AND DATA REDUCTION

WR 137 was observed with *XMM-Newton* on 2013 Oct 9 (Observation ID 0720600101) with a nominal exposure of  $\sim 50$  ks. The source was detected (see Fig. 1) but it was not very bright in X-rays, thus, our analysis is based on the data from the European Photon Imaging Camera (EPIC) having one pn and two MOS detectors<sup>1</sup>. For the data reduction, we made use of the *XMM-Newton* SAS<sup>2</sup> 12.0.1 data analysis software. The SAS pipeline processing scripts *emproc* and *epproc* were executed to incorporate the most recent calibration files (as of 2014 June 4). The data were then filtered for high X-ray background following the instructions in the SAS documentation. The SAS procedures *rmfgen* and *arfgen* were adopted to generate the corresponding response matrix

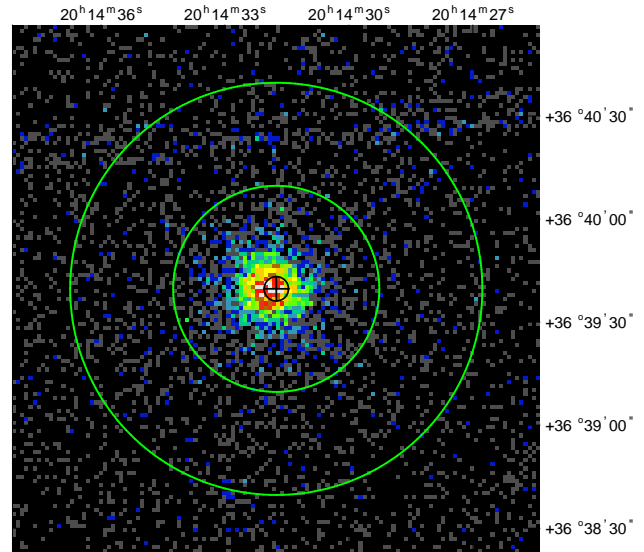


**Figure 1.** The raw EPIC-pn image of WR 137 in the 0.2 - 10 keV energy band with the spectral extraction regions. The source spectrum was extracted from the central circle, while the background spectrum was extracted from adjacent annulus. The circled plus sign gives the optical position of WR 137 (SIMBAD).

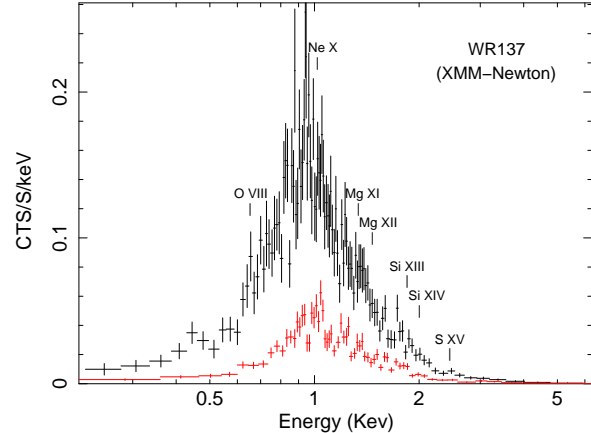


**Figure 2.** The background-subtracted spectra of WR 137 rebinned to have a minimum of 30 counts per bin. Positions of some, usually strong, emission  $L_\alpha$  and  $K_\alpha$  line features of various ionic species are marked. The pn (upper curve) and MOS (lower curve) spectra are shown in black and red colour, respectively.

files and ancillary response files for each spectrum. The MOS spectrum in our analysis is the sum of the spectra from the two MOS detectors. The extracted spectra (0.2 - 10 keV) of WR 137 had  $\sim 3427$  source counts in the 26.8-ks pn effective exposure and  $\sim 2366$  source counts in the 32.6-ks MOS effective exposure.

Also, we constructed the pn and MOS1,2 background-subtracted light curves of WR 137. On a timescale less than 35 ks and time bins between 100 and 1000 s, the X-ray light curves were statistically consistent with a constant flux: adopting  $\chi^2$  fitting, the light curves were fitted with a constant and the goodness-of-fit was  $\geq 0.70$ .

Thus, our study was centred around the global analy-

<sup>1</sup> see § 3.3 in the *XMM-Newton* Users Handbook, [http://xmm.esac.esa.int/external/xmm\\_user\\_support/documentation/uhb](http://xmm.esac.esa.int/external/xmm_user_support/documentation/uhb)

<sup>2</sup> Science Analysis Software, <http://xmm.esac.esa.int/sas>

sis of the *XMM-Newton* spectra of WR 137. For that, we used standard as well as custom models in version 11.3.2 of XSPEC (Arnaud 1996).

## 4 RESULTS

The X-ray spectra of WR 137 are shown in Fig. 2. It is worth noting that the emission line features are rather weak. This is a bit in contrast with the situation in the X-ray spectrum of another dust maker, WR 48a (see fig. 2 in Zhekov et al. 2011). We note that the data for WR 137 and WR 48a were taken with exactly the same instrumentation (*XMM-Newton* EPIC).

To derive the properties of the X-ray emitting plasma in WR 137, we adopted global spectral fitting to its *XMM-Newton* spectra. The EPIC-pn and EPIC-MOS spectra were fitted simultaneously sharing identical model parameters. We used discrete-temperature models in XSPEC that assume plasma in collisional ionization equilibrium (CIE; model *vapec*) as well as such that assume plasma with non-equilibrium ionization (NEI; model *vpshock*). The adopted set of abundances is that from van der Hucht et al. (1986) typical for the WC stars (by number): H = 0.00, He = 0.618, C = 0.248, N = 0.00, O = 0.120, Ne =  $1.15 \times 10^{-2}$ , Mg =  $1.68 \times 10^{-3}$ , Si =  $4.23 \times 10^{-4}$ , S =  $9.40 \times 10^{-5}$ , Fe =  $2.36 \times 10^{-4}$ . To improve the quality of the fits, the O, Ne, Mg, Si and Fe abundances were allowed to vary. The emission plasma components were subject to common X-ray absorption (model *wabs* in XSPEC).

We performed one- and two-temperature plasma model fits. Table 1 and Figure 3 present the corresponding results from the fits to the *XMM-Newton* spectra of WR 137. A few things are worth mentioning.

We see that the one-temperature plasma models, with not very high temperature ( $kT \approx 0.8$  keV), give statistically acceptable fits to the X-ray spectra of WR 137 but they slightly underestimate its X-ray emission at energies above 3 keV. On the other hand, the spectral fits of the two-temperature plasma models do not have this caveat and the quality of the fits improves: the  $\chi^2$  value decreases by 25-30%. Thus, we will further focus mostly on the results from these model fits.

An interesting feature of the two-temperature NEI model fit is the relatively high value of the ionization age (model parameter  $\tau$ ). We note that both emission components have such high values which is indicative of plasma with ionization state close to CIE.

The X-ray absorption, as derived from the two-temperature fits, is in general consistent with the optical extinction to WR 137 (see Section 2). Namely, it is only by 15-25% higher than the latter if we adopt the Gorenstein (1975) conversion. But the result may indicate some extra absorption ( $\sim 60\%$ ) if a more recent conversion is used (Vuong et al. 2003, Getman et al. 2005; see Section 2).

To explore this a bit in detail, we ran the same two-temperature CIE and NEI models with two-component X-ray absorption. The first component was fixed to the value corresponding to the optical extinction (the ISM absorption component) and the second component (the wind absorption component) was allowed to vary. For physical consistency, the wind absorption component shared the same

abundances with the emission plasma components in the fits. These fits were statistically as good as the ones with a single X-ray absorption component (Table 1) with  $\chi^2/\text{dof} = 119/162$ ; 118/160 for the CIE and NEI models, respectively. The helium column density of the wind absorption was  $N_{\text{He},\text{wind}} = (0.5 - 1.0) \times 10^{19} \text{ cm}^{-2}$ . Such a low value of the wind-absorption column density shows that the X-ray emission region in WR 137 is *not* located deep in the WC wind. For comparison, the radial helium column density of the WC wind from infinity to a distance  $R_{\text{au}}$  (given in au) is  $N_{\text{He},\text{wind},\text{rad.}} = 2.58 \times 10^{21} R_{\text{au}}^{-1} \text{ cm}^{-2}$ , if adopting the wind parameters of WR 137 (Section 2) and the WC abundances. The column density derived from the fits then puts the X-ray emission region at a very large (and unrealistic) distance of more than 200 au from the WC star in WR 137. This is likely a sign that the X-ray small extra (or wind) absorption is a result from the use of simple models in the spectral fits. Thus, it is conclusive that the X-ray absorption of WR 137 is consistent with the optical extinction towards this object.

We note that in general the X-ray spectrum of WR 137 does not show strong emission line features (Fig. 2). As already noted, the second component in the two-temperature optically-thin plasma models mostly contributed to the relatively weak continuum at energies higher than 3 keV. We ran two-component fits with an optically-thin plasma model (*vapec* or *vpshock*) as a first component and a continuum model (a black body or a power-law model) as a second component. In statistical sense, these fits proved to be equally successful as the two-temperature optically-thin plasma models.

The two-component fit, that is a sum of an optically-thin plasma and a black body model subject to common absorption, had  $\chi^2/\text{dof} = 119/162$ ,  $N_H = 4.82^{+0.26}_{-0.21} \times 10^{21} \text{ cm}^{-2}$ ,  $kT_1 = 0.41^{+0.02}_{-0.02} \text{ keV}$ ,  $kT_{\text{BB}} = 0.74^{+0.03}_{-0.02} \text{ keV}$ . And, the corresponding fit with a power-law model as the second component had  $\chi^2/\text{dof} = 124/162$ ,  $N_H = 4.70^{+0.36}_{-0.25} \times 10^{21} \text{ cm}^{-2}$ ,  $kT_1 = 0.40^{+0.02}_{-0.03} \text{ keV}$ ,  $\Gamma = 2.80^{+0.34}_{-0.17}$ , where  $\Gamma$  is the photon power-law index ( $F_{\text{PL}} \propto E^{-[\Gamma-1]}$ ). It is interesting to note that the values of the X-ray absorption and the plasma temperature of the first component are practically identical to the corresponding values from the fits with the two-temperature optically-thin plasma models (see Table 1).

Finally, using the unabsorbed fluxes (two-temperature models in Table 1) and a distance of 2.38 kpc (Section 2) we see that the X-ray luminosity of WR 137 is not very high:  $\log L_X = 32.76 - 32.83$  ( $L_X$  in  $\text{ergs s}^{-1}$ ). In fact, its value is close to that typical for close WR+O binaries (e.g., Zhekov 2012) and it is also similar to the upper values for the range of X-ray luminosities amongst the presumably single WN stars (Skinner et al. 2010). On the other hand, it is by one-two orders of magnitude less than the X-ray luminosity of other dust makers as WR140 (Zhekov & Skinner 2000, Pollock et al. 2005) and WR 48a (Zhekov et al. 2011).

## 5 DISCUSSION

Some of the basic results from the analysis of the X-ray spectra of the dust maker WR 137 are as follows. The X-ray absorption is in general consistent with the optical extinction to WR 137. The relatively hot plasma is present in the X-ray emitting region but its emission does not dominate the

**Table 1.** Global Spectral Model Results

Parameter	2T vapec	2T vpshock	1T vapec	1T vpshock
$\chi^2/\text{dof}$	119/162	118/160	163/164	155/163
$N_H$ ( $10^{21} \text{ cm}^{-2}$ )	$4.66^{+0.25}_{-0.16}$	$5.15^{+0.58}_{-0.43}$	$3.51^{+0.15}_{-0.15}$	$6.30^{+0.24}_{-0.35}$
$kT_1$ (keV)	$0.40^{+0.01}_{-0.02}$	$0.37^{+0.05}_{-0.02}$	$0.79^{+0.03}_{-0.03}$	$0.82^{+0.04}_{-0.03}$
$kT_2$ (keV)	$2.11^{+0.38}_{-0.23}$	$2.24^{+0.51}_{-0.42}$		
$EM_1$ ( $10^{54} \text{ cm}^{-3}$ )	$2.09^{+0.19}_{-0.10}$	$2.42^{+0.53}_{-0.43}$	$1.57^{+0.13}_{-0.12}$	$1.95^{+0.18}_{-0.26}$
$EM_2$ ( $10^{54} \text{ cm}^{-3}$ )	$0.51^{+0.09}_{-0.03}$	$0.50^{+0.10}_{-0.10}$		
$\tau_1$ ( $10^{12} \text{ cm}^{-3} \text{ s}$ )		$8.62^{+41.4}_{-5.54}$		$0.21^{+0.05}_{-0.04}$
$\tau_2$ ( $10^{12} \text{ cm}^{-3} \text{ s}$ )		$0.91^{+49.1}_{-0.58}$		
O	$0.03^{+0.02}_{-0.01}$	$0.03^{+0.01}_{-0.01}$	$0.08^{+0.03}_{-0.03}$	$0.05^{+0.01}_{-0.01}$
Ne	$0.12^{+0.02}_{-0.02}$	$0.10^{+0.03}_{-0.02}$	$0.11^{+0.03}_{-0.03}$	$0.07^{+0.01}_{-0.01}$
Mg	$0.07^{+0.04}_{-0.04}$	$0.06^{+0.02}_{-0.03}$	$0.02^{+0.03}_{-0.02}$	$0.04^{+0.01}_{-0.01}$
Si	$0.48^{+0.20}_{-0.20}$	$0.34^{+0.14}_{-0.14}$	$0.06^{+0.06}_{-0.06}$	$0.05^{+0.05}_{-0.05}$
Fe	$0.23^{+0.09}_{-0.08}$	$0.26^{+0.13}_{-0.10}$	$0.36^{+0.06}_{-0.05}$	$0.49^{+0.11}_{-0.20}$
$F_X$ ( $10^{-13} \text{ ergs cm}^{-2} \text{ s}^{-1}$ )	2.61 (8.37)	2.62 (10.0)	2.38 (5.42)	2.41 (16.0)
$F_{X,hot}$ ( $10^{-13} \text{ ergs cm}^{-2} \text{ s}^{-1}$ )	1.01 (1.58)	1.10 (2.03)		

Note – Results from simultaneous fits to the EPIC spectra of WR 137. Tabulated quantities are the neutral hydrogen absorption column density ( $N_H$ ), plasma temperature (kT), emission measure ( $EM = \int n_e n_H dV$ ) for a reference distance of  $d = 2.38$  kpc, shock ionization age ( $\tau = n_e t$ ), the absorbed X-ray flux ( $F_X$ ) in the 0.5 - 10 keV range followed in parentheses by the unabsorbed value ( $F_{X,hot}$  denotes the higher-temperature component,  $kT_2$ ). The derived abundances are with respect to the typical WC abundances (van der Hucht et al. 1986). Errors are the  $1\sigma$  values from the fits.

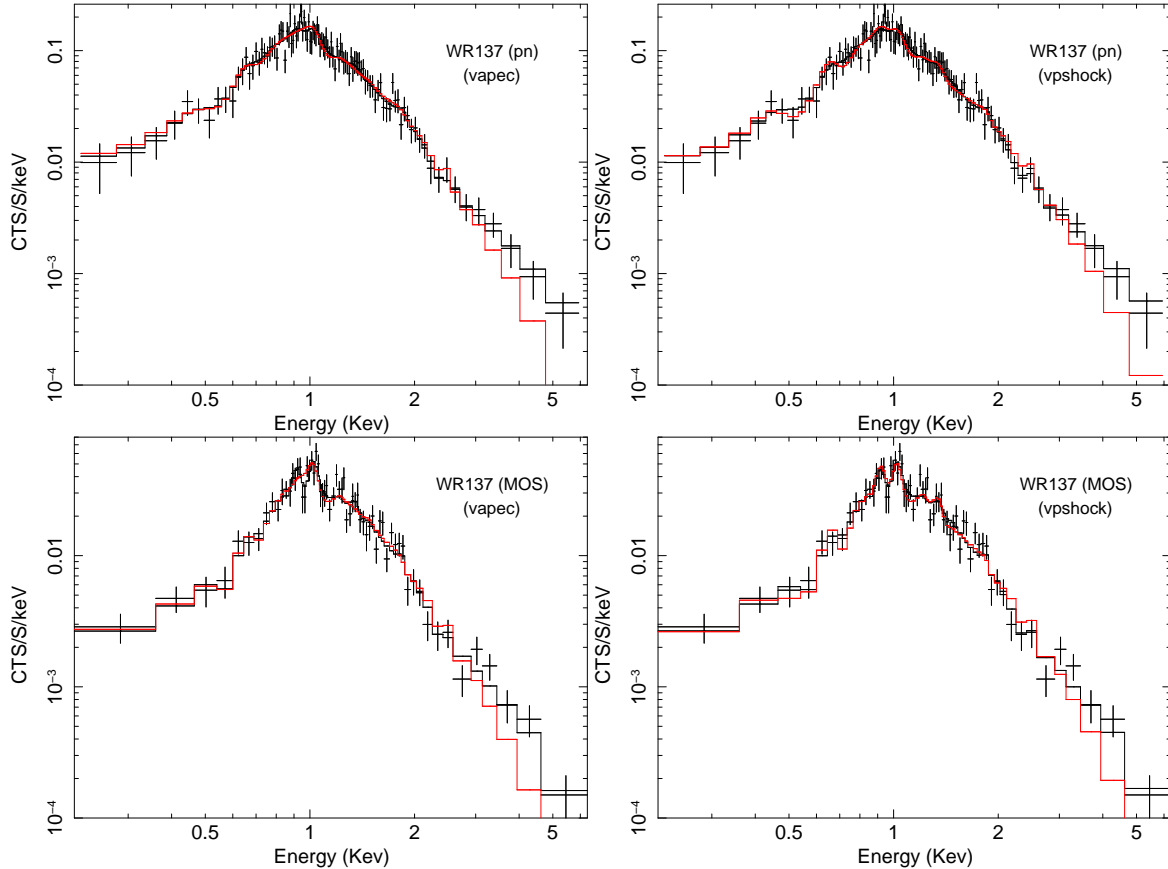


**Figure 3.** The background-subtracted spectra of WR 137 and the discrete-temperature model fits (Table 1): ‘vapec’ and ‘vpshock’ denote the case of optically-thin plasma or plane-parallel shock emission, respectively. In each panel, the two- and one-temperature model spectra are shown with a stepped line in black and red colour, respectively. The spectra were re-binned to have a minimum of 30 counts per bin.

X-ray spectrum of this object. The X-ray luminosity is not very high: it is considerably lower than that of dust makers with well studied X-ray emission (WR 48a and WR 140).

It is worth recalling that CSWs in wide WR+O binaries play an important role for the physics of episodic dust makers. For example, the strong and variable infrared, X-ray and non-thermal radio emission of the prototype EDM, WR 140, can find an explanation in the CSW paradigm (Williams et al. 1990). Studies of another EDM, WR 48a, suggest that CSWs should play an important role for its infrared and X-ray emission (Williams et al. 2012; Zhekov et al. 2011; 2014) although the physical picture may be more complex than that (see Zhekov et al. 2014). It is thus important to explore the CSW picture for WR 137 in some detail as well.

### 5.1 CSW model spectra

To model the X-ray spectra from CSWs in WR 137, we used the models by Zhekov & Skinner (2000) and Zhekov (2007) that allow for different electron and ion temperatures and the NEI effects. These models are based on the hydrodynamic model of adiabatic CSWs by Myasnikov & Zhekov (1993). The latter assumes spherical symmetry of the stellar winds that have reached their terminal velocity before they collide. It also allows for different chemical abundances in the CSW region occupied by the shocked WR and O stellar winds, respectively. Thus, in all the spectral fits the chemical abundances of the shocked O-star wind were solar (Anders & Grevesse 1989) while those of the shocked WR-star wind were typical for the WC stars (van der Hucht et al. 1986). The latter were also allowed to vary in our fits to the X-ray spectra of WR 137 in XSPEC.

We note that the basic input parameters for the CSW hydrodynamic model in WR+O binaries are the mass loss and velocity of the stellar winds of the binary components and the binary separation. The former define a dimensionless parameter  $\Lambda = (\dot{M}_{WR}V_{WR})/(\dot{M}_OV_O)$  which determines the shape and the structure of the CSW interaction region (Myasnikov & Zhekov 1993).

For the wind parameters of the WC star in WR 137, we adopted  $V_{WR} = 1885 \text{ km s}^{-1}$  and  $\dot{M}_{WR} = 3 \times 10^{-5} M_{\odot} \text{ yr}^{-1}$  (Section 2). Using the orbital elements and inclination angle of  $i = 67^\circ$  (see Lefèvre et al. 2005 and table 4 therein) and Kepler's third law, we derived a mean binary separation of  $a = 2.41 \times 10^{14} \text{ cm}$ . We note that the time of the *XMM-Newton* observation (Section 3) corresponds to an orbital phase of  $\phi = 0.338$  which for an orbital ellipticity of  $e = 0.178$  translates into a binary separation of  $1.113 \times a$ . Since the wind parameters of the O star in WR 137 are not observationally constrained, we adopted the following approach in our procedure for modelling the CSW spectra of this object. Namely, we assumed that the terminal wind velocity of the O star is equal to that of the WC star in the system ( $V_O = V_{WR} = 1885 \text{ km s}^{-1}$ ). We explored a range of values for the  $\Lambda$ -parameter:  $\Lambda = 16, 25, 36$  (these correspond to  $\dot{M}_O = 1.88, 1.20, 0.83 \times 10^{-6} M_{\odot} \text{ yr}^{-1}$ , respectively). It is worth noting that the exact values of the O-star wind parameters are not quite important for the X-ray emission from CSWs in WR+O binaries because of the dominant contribution of the shocked WR-wind gas (Myasnikov & Zhekov 1993). Anticipating the results from

the CSW spectral fits, we note that the contribution from the shocked O-star wind to the entire X-ray emission from CSWs in WR 137 was only 1-2% of the observed X-ray flux.

In order to explore the wealth of physical processes that might be important for the X-ray emission from CSWs in wide WR+O binaries as WR 137, we ran a series of models that consider hot plasma in collisional ionization equilibrium or with non-equilibrium ionization, and we also considered the case of partial heating of the electrons at the shock front (non-equal electron and ion temperatures). We recall that the latter is adopted through the  $\beta$ -parameter that gives the ratio of the electron and mean plasma temperatures ( $\beta = T_e/T$ ) at the shock front and the electron and ion temperatures equilibrate downstream behind the shock (see Zhekov & Skinner 2000 for details).

We fitted the X-ray spectra of WR 137 in XSPEC with the CSW model spectra using the nominal values of the wind parameters as described above. In all the cases under consideration (different values of the  $\Lambda$ -parameter), the theoretical spectra matched the shape of the observed spectra but they overestimated the observed flux by about two orders of magnitude. In other words, the nominal wind parameters suggest way too high an emission measure of the CSW region in WR 137.

We note that the emission measure is proportional to the square of the plasma density ( $EM \propto n^2V$ ,  $n$  is the number density,  $V$  is the volume), therefore, to the square of the stellar wind mass loss. Alternatively, the emission measure is reversely proportional to the binary separation ( $n \propto 1/a^2$  and  $V \propto a^3$ , therefore  $EM \propto 1/a$ ) which suggests a much larger and unrealistic binary separation for the WR 137 binary period of 4766 days (Section 2) in order to synchronize the emission measure with the observational requirements.

We thus re-ran the CSW spectral models by adopting the correspondingly reduced mass losses in order to match the observed flux from WR 137. We also ran CSW spectral models with a reduced carbon abundance to see its effect on the required mass-loss reduction factor. Some fit results ( $\Lambda = 36$ ) are given in Table 2 and in Figure 4.

We see that the CSW spectral models match acceptably well the observed X-ray spectra of WR 137. This is valid for all the cases under consideration: such with the carbon abundance typical for the WC stars or with the reduced one (respectively models A1-through-A4 and B1-through-B4 in Table 2); such with CIE plasma or plasma in NEI; such with plasma having different electron and ion temperatures. However, the models with complete temperature equalization (models A1, A2, B1 and B2) have the caveat of slightly overestimating the X-ray emission from WR 137 at energies above  $\sim 3 \text{ keV}$  (e.g., Fig.4). This is a likely indication of presence of X-ray emission plasmas in the CSW region hotter than required by the *XMM-Newton* spectra. Understandably, the models with a partial electron heating at the shock front (models A3, A4, B3 and B4 all having  $\beta = T_e/T = 0.1$ ) provide a better match to the observed spectra. In fact, we ran CSW models with various values for the  $\beta$ -parameter and the result was that all the models with  $\beta \leq 0.1$  provided about the same quality of the CSW spectral fits while those with higher degree of temperature equalization ( $\beta = 0.2-1$ ) started to show an excess emission at energies above  $\sim 3 \text{ keV}$ .

For all the CSW model fits, the values of the X-ray

**Table 2.** CSW Spectral Model Results

Parameter	C / He = 0.4				C / He = 0.1			
	CIE (A1)	NEI (A2)	$T_{ei}+CIE$ (A3)	$T_{ei}+NEI$ (A4)	CIE (B1)	NEI (B2)	$T_{ei}+CIE$ (B3)	$T_{ei}+NEI$ (B4)
Reduced $\dot{M}$ by a factor of	12.7	12.7	9.5	9.5	9.5	9.5	7.7	7.7
$\chi^2/\text{dof}$	190/165	176/165	143/165	142/165	190/165	176/165	157/165	158/165
$N_H$ ( $10^{21} \text{ cm}^{-2}$ )	$2.76^{+0.23}_{-0.18}$	$4.20^{+0.20}_{-0.17}$	$3.43^{+0.20}_{-0.17}$	$4.69^{+0.20}_{-0.17}$	$2.76^{+0.27}_{-0.21}$	$3.74^{+0.23}_{-0.19}$	$3.15^{+0.23}_{-0.19}$	$4.14^{+0.23}_{-0.19}$
O	$0.16^{+0.07}_{-0.05}$	$0.13^{+0.03}_{-0.03}$	$0.08^{+0.03}_{-0.03}$	$0.09^{+0.02}_{-0.02}$	$0.05^{+0.03}_{-0.02}$	$0.04^{+0.01}_{-0.01}$	$0.03^{+0.01}_{-0.01}$	$0.03^{+0.01}_{-0.01}$
Ne	$0.62^{+0.13}_{-0.11}$	$0.17^{+0.07}_{-0.07}$	$0.23^{+0.05}_{-0.05}$	$0.13^{+0.04}_{-0.04}$	$0.21^{+0.05}_{-0.04}$	$0.08^{+0.03}_{-0.03}$	$0.10^{+0.02}_{-0.02}$	$0.06^{+0.02}_{-0.02}$
Mg	$1.17^{+0.24}_{-0.20}$	$0.47^{+0.08}_{-0.08}$	$0.28^{+0.08}_{-0.07}$	$0.19^{+0.05}_{-0.04}$	$0.43^{+0.08}_{-0.07}$	$0.22^{+0.04}_{-0.03}$	$0.17^{+0.04}_{-0.03}$	$0.12^{+0.02}_{-0.02}$
Si	$1.81^{+0.55}_{-0.48}$	$1.10^{+0.25}_{-0.23}$	$0.41^{+0.21}_{-0.19}$	$0.39^{+0.14}_{-0.13}$	$0.69^{+0.20}_{-0.15}$	$0.50^{+0.11}_{-0.10}$	$0.27^{+0.09}_{-0.08}$	$0.26^{+0.07}_{-0.06}$
Fe	$2.61^{+0.56}_{-0.41}$	$4.01^{+0.60}_{-0.52}$	$1.00^{+0.19}_{-0.16}$	$1.71^{+0.27}_{-0.24}$	$0.90^{+0.21}_{-0.15}$	$1.40^{+0.21}_{-0.18}$	$0.46^{+0.09}_{-0.07}$	$0.76^{+0.12}_{-0.10}$
<i>norm</i>	$0.97^{+0.09}_{-0.10}$	$1.00^{+0.08}_{-0.08}$	$0.99^{+0.07}_{-0.07}$	$0.99^{+0.06}_{-0.06}$	$1.09^{+0.10}_{-0.11}$	$1.06^{+0.08}_{-0.08}$	$1.09^{+0.08}_{-0.08}$	$1.05^{+0.07}_{-0.07}$
$F_X$ ( $10^{-13} \text{ ergs cm}^{-2} \text{ s}^{-1}$ )	2.92 (4.92)	2.94 (7.57)	2.66 (5.60)	2.66 (8.68)	2.90 (4.92)	2.90 (6.52)	2.69 (5.23)	2.68 (7.20)

Note – Results from simultaneous fits to the EPIC spectra of WR 137 using model spectra from the CSW hydrodynamic simulations. Two type of models were considered: one with the WC standard carbon abundance (C / He = 0.4) and another with a reduced carbon abundance (C / He = 0.1). Four versions of each model were adopted (A1 through A4 and B1 through B4): with collisional ionization equilibrium (CIE), with non-equilibrium ionization (NEI) as well as their versions that take into account the different electron and ion temperatures ( $T_{ei}+CIE$  and  $T_{ei}+NEI$ ). For each model, given is the factor by which the mass-loss rates of the stellar winds were reduced (see Section 5.1 for details). Tabulated quantities are the neutral hydrogen absorption column density ( $N_H$ ), the O, Ne, Mg, Si and Fe abundances, the normalization parameter (*norm*) and the absorbed X-ray flux ( $F_X$ ) in the 0.5 - 10 keV range followed in parentheses by the unabsorbed value. The *norm* parameter is a dimensionless quantity that gives the ratio of observed to theoretical fluxes. A value of *norm* = 1.0 indicates a perfect match between the observed count rate and that predicted by the model. The derived abundances are with respect to the typical WC abundances (van der Hucht et al. 1986). Errors are the  $1\sigma$  values from the fits.

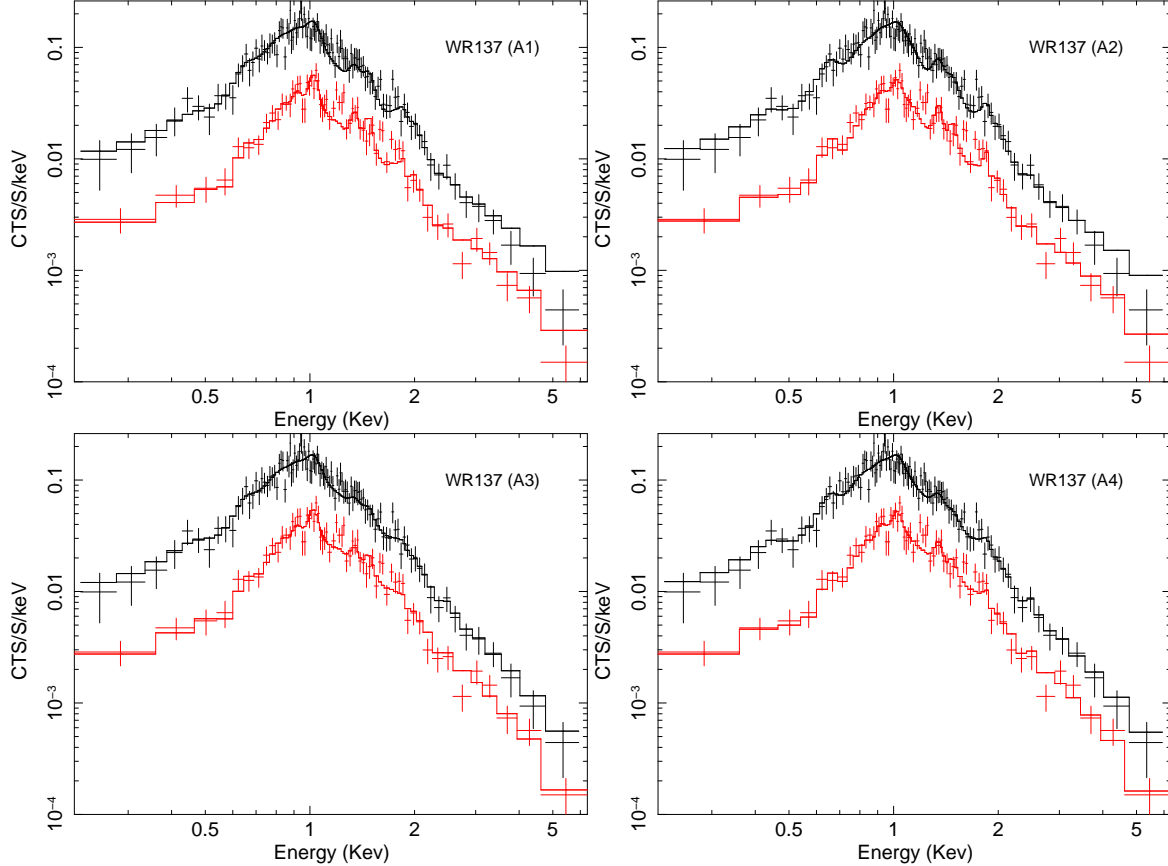


**Figure 4.** The background-subtracted spectra of WR 137 overlaid with the CSW model fits. The labels A1, A2, A3 and A4 denote the corresponding models from Table 2. In each panel, the pn (upper curve) and MOS (lower curve) spectra are shown in black and red colour, respectively. The spectra were re-binned to have a minimum of 30 counts per bin.



absorption ( $N_H$ ) are in general consistent with the optical extinction to WR 137 (Section 2). This is in fact in accord with the CSW picture in wide binaries in which the interaction region is not located deep in the stellar winds, thus, no appreciable wind absorption should be expected.

But, the most interesting result from adopting the CSW picture in the case of WR 137 is probably the requirement of relatively low mass loss in order to match the observed X-ray flux from this object. The mass loss needs be reduced by about one order of magnitude with respect to the currently accepted value for WR 137 (Section 2). Such a low figure ( $\dot{M}_{WR} \approx [2 - 4] \times 10^{-6} M_\odot \text{ yr}^{-1}$ ) is quite atypical for a WR star, so, could it indicate a very efficient wind clumping even at large distance from this WC star? That is, the stellar wind in WR 137 might be a two-component flow and only the smooth (less massive) component is playing a role for the colliding stellar winds in this binary. On the other hand, the requirement for a very low mass loss might be a sign that the X-ray emission from WR 137 is due to some other mechanism rather than to CSWs in a wide WR+O binary.

Similar indication may come from the appreciable difference between the values of the X-ray luminosity of WR 137 as deduced from the *XMM-Newton* data,  $L_X = 4.5 \times 10^{32} \text{ ergs s}^{-1}$ , (the mean for the values in Table 2) and from the previous observations:  $L_X = 2.8 \times 10^{32} \text{ ergs s}^{-1}$  with *Einstein*;  $L_X = 1.1 \times 10^{32} \text{ ergs s}^{-1}$  with *ROSAT* (the values cited in Section 2 were rescaled to the distance of 2.38 kpc adopted in this study). This luminosity difference is hard to explain by the different pass-bands of the X-ray telescopes. On the other hand, it is worth noting that such a difference cannot be due solely to the orbital changes since the binary separation was not too different in these three occasions. Namely, the orbital phase and the corresponding binary separation were  $\phi = 0.338$  and  $1.113 \times a$  (*XMM-Newton*);  $\phi = 0.698$  and  $1.083 \times a$  (*ROSAT*);  $\phi = 0.775$  and  $1.004 \times a$  (*Einstein*), where  $a$  is the mean orbital separation. To find an explanation of this luminosity variability, we might need some physical reason (mechanism) for such changes that may go beyond the CSW picture in WR 137. However, we have to keep in mind that the *Einstein* and *ROSAT* data on WR 137 have very limited photon statistics. Future observations with good quality are indeed needed to check this result which will help us improve our understanding of the X-ray production mechanism in WR 137.

## 5.2 Comparison with other EDMs

Since WR 137 is one of the seven originally proposed episodic dust makers (Williams 1995), it is interesting to compare its global properties with those of other EDMs. We recall that the global properties of the prototype EDM, WR 140, in the infrared, radio and X-ray spectral domains are best explained in the framework of the CSW picture in a wide WR+O binary system (Williams et al. 1990). With WR 137 having an X-ray spectrum with good quality, there are now three EDMs that were studied in those spectral domains in some detail: WR 48a, WR 137 and WR 140.

The IR emission is basic for EDMs: this is the spectral domain where the classification of these objects came from (Williams 1995). The IR light curve of WR 137 (Williams et al. 2001) is quite similar to that of WR 48a (Williams et al. 2012). Both LCs show a gradual

increase and then decrease between the minimum and maximum values of their IR emission. They show some ‘mini eruptions’ as well. In contrast, the IR emission of the prototype EDM, WR 140, surges to a maximum in a short period of time (due to the sudden onset of dust formation) and then decreases more slowly to its minimum value (Williams et al. 1990).

The radio properties of these three EDMs are not uniform either. WR 140 is a strong and variable non-thermal radio source (Williams et al. 1990; White & Becker 1995; Dougherty et al. 2005). WR 48a is very likely a thermal (and variable) radio source (Hindson et al. 2012; Zhekov et al. 2014). WR 137 was first classified as a thermal radio source by Abbott et al. (1986). Later, Dougherty & Williams (2000) listed it also as a non-thermal radio source, although this classification was based only on a private communication. Thus, in detail radio studies of WR 137 are needed to settle the origin of its radio emission.

On the other hand, the X-ray studies of EDMs are very important since they provide information about the properties of the CSW region in these presumable wide WR+O binaries. In X-rays, the most interesting feature is probably that the X-ray luminosity of WR 137 is appreciably lower than that of WR 48a and WR 140 (see Section 4). While the orbital elements and the stellar wind parameters of WR 48a are not well constrained (Zhekov et al. 2014), the prototype EDM, WR 140, is well studied in this respect. Thus, we can have a simple comparison between the X-ray luminosities of WR 140 and WR 137 in the framework of the CSW picture.

Namely, there exists a scaling law for the CSW X-ray luminosity with the mass-loss rate ( $\dot{M}$ ), wind velocity ( $v$ ) and binary separation ( $a$ ):  $L_X \propto \dot{M}^2 v^{-3} a^{-1}$  (Luo et al. 1990; Myasnikov & Zhekov 1993). We note that the stellar wind parameters and the binary separations (or orbital periods) of WR 137 and WR 140 are not strikingly different (see Section 2 here and table 3 in Williams et al. 1990). Based on this scaling law, it is then *not* anticipated that the X-ray luminosities of these objects will differ considerably (mean  $L_X[\text{WR 137}] / \text{mean } L_X[\text{WR 140}] \approx 0.89$ ). Nevertheless, we see that the X-ray luminosity of WR 137 is at least one order of magnitude less than that of WR 140:  $L_X(\text{WR 137}) \leq 10^{33} \text{ ergs s}^{-1}$  (Section 4) vs.  $L_X(\text{WR 140}) \geq 10^{34} \text{ ergs s}^{-1}$  (Zhekov & Skinner 2000; Pollock et al. 2005). In order to match the observed flux (and the X-ray luminosity) of WR 137, an appreciable reduction of the mass-loss rate was needed in the framework of the CSW picture. As mentioned in Section 5.1, this raises questions and even doubts about the overall validity of the CSW paradigm for the case of WR 137. Along these lines, we mention that the X-ray spectrum of WR 137 could be well represented by a two-component emission: one component is from thermal plasma and the second one is a ‘pure’ continuum (black-body or power-law) emission (see Section 4).

However, we have to keep in mind that the relatively strong X-ray emission from WR 137 and the really strong one from WR 48a and WR 140 are a clear sign that the binary nature of these objects provides some suitable conditions for an efficient X-ray production mechanism to operate in them. This is so since these three objects (and all the EDMs as well) are carbon-rich Wolf-Rayet stars. And, we recall that all the pointed observations of presumably single WC stars resulted in non-detections (Osino et al. 2003;

Skinner et al. 2006). Thus, single WCs are likely very faint or X-ray quite objects, opposite to what is observed from WR 48a, WR 137 and WR 140.

In summary, we note that although the CSW picture is very successful in explaining the global properties of the prototype EDM WR 140, we need to find some more observational support for its validity in such objects like WR 137 and WR 48a. We believe that studies of other EDMs, yet unobserved in X-rays, will be also very important to help us understand the physics of this extremely interesting phenomenon: episodic dust formation and its relation to colliding stellar winds in wide WR+O binaries.

## 6 CONCLUSIONS

In this work, we presented the *XMM-Newton* data of WR 137 which provide the first X-ray spectra with good quality of this episodic dust maker. The basic results and conclusions are as follows.

(i) WR 137 is a relatively strong X-ray source ( $\log L_X = 32.76 - 32.83$ ,  $L_X$  in  $\text{ergs s}^{-1}$ ) with relatively weak emission-line features in its X-ray spectrum. It shows no short-term (within 35 ks) X-ray variability.

(ii) Discrete-temperature global spectral fits show that the X-ray spectra of WR 137 are well matched by a two-temperature optically-thin plasma emission ( $kT_1 \sim 0.4$  keV and  $kT_2 \sim 2.2$  keV). However, its X-ray emission is also well represented by a two-component model whose first component is from a thermal plasma and the second component is a ‘pure’ continuum (black body or power-law) emission.

(iii) Colliding stellar wind model spectra match well the shape of the observed X-ray spectrum of WR 137. However, they overestimate the observed flux (emission measure) by about two orders of magnitude. To reconcile the model predictions with observations, the mass loss of WR 137 must be reduced considerably with respect to its currently accepted value. Such a low mass loss ( $\dot{M}_{WR} \approx [2-4] \times 10^{-6} M_\odot \text{ yr}^{-1}$ ) may indicate a very efficient wind clumping even at large distance from this WC star. Alternatively, it might be a sign that some other X-ray production mechanism is at play in WR 137 rather than CSWs in a wide WR+O binary.

(iv) The X-ray absorption, derived from the spectral fits, is consistent with the optical extinction to WR 137. This is valid both for the discrete-temperature and for the CSW spectral models.

(v) There are now three EDMs (WR 48a, WR 137 and WR 140) that have X-ray spectra with good quality. Since the X-ray properties of these objects are not quite uniform, X-ray studies of the entire group of EDMs will be very helpful for understanding the physics of episodic dust makers and to establish whether colliding stellar winds is their basic X-ray production mechanism.

## 7 ACKNOWLEDGEMENTS

This research has made use of data and/or software provided by the High Energy Astrophysics Science Archive Research Center (HEASARC), which is a service of the Astrophysics Science Division at NASA/GSFC and the High Energy Astrophysics Division of the Smithsonian Astrophysical Ob-

servatory. This research has made use of the NASA’s Astrophysics Data System, and the SIMBAD astronomical data base, operated by CDS at Strasbourg, France. The author thanks an anonymous referee for helpful comments and suggestions.

## REFERENCES

- Abbott D.C., Biegging J.H., Churchwell E., Torres A.V. 1986, *ApJ*, 303, 239
- Anders E., & Grevesse N., 1989, *Geochimica et Cosmochimica Acta*, 53, 19
- Arnaud, K.A. 1996, in Jacoby G., Barnes, J. eds., *ASP Conf. Ser. Vol. 101, Astronomical Data Analysis Software and Systems*, Astron. Soc. Pac., San Francisco, 17
- Cherepashchuk, A.M. 1976, *Soviet Astronomy Letters*, 2, 138
- Dougherty, S.M., Beasley, A.J., Claussen, M.J., Zauderer, B.A., & Bolingbroke, N.J. 2005, *ApJ*, 623, 447
- Dougherty, S.M., & Williams, P.M. 2000, *MNRAS*, 319, 1005
- Getman, K.V., Feigelson, E.D., Grosso, N., McCaughrean, M.J., Micela, G., Broos, P., Garmire, G., & Townsley, L. 2005, *ApJS*, 160, 363
- Gorenstein, P. 1975, *ApJ*, 198, 95
- Hindson, L., Thompson, M. A., Urquhart, J. S., Faimali, A., Clark, J. S., & Davies, B. 2012, *MNRAS*, 421, 3418
- Lefèvre, L., Marchenko, S.V., Lépine, S. et al. 2005, *MNRAS*, 360, 141
- Luo, D., McCray, R., & MacLow, M.-M. 1990, *ApJ*, 362, 267
- Myasnikov, A.V. & Zhekov, S.A. 1993, *MNRAS*, 260, 221
- Nugis, T., Crowther, P.A. & Willis, A.J. 1998, *A&A*, 333, 956
- Oskinova, L.M, Ignace, R., Hamann, W.-R., Pollock, A.M.T., & Brown, J.C. 2003, *A&A*, 402, 755
- Pollock, A.M.T. 1987, *ApJ*, 320, 283
- Pollock, A.M.T., Haberl, F., & Corcoran, M.F. 1995, in van der Hucht K.L., Williams P.M., eds. *Proc. IAU Symp 163, Wolf-Rayet Stars: Binaries, Colliding Winds, Evolution*, Kluwer, Dordrecht, p. 512
- Pollock, A.M.T., Corcoran, M.F., Stevens, I.R., & Williams, P.M. 2005, *ApJ*, 629, 482
- Prilutskii, O.F. & Usov, V.V. 1976, *Soviet Astronomy*, 20, 2
- Skinner, S.L., Güdel, M., Schmutz, W. & Zhekov, S.A. 2006, *Ap&SS*, 304, 97
- Skinner S.L., Zhekov S.A., Güdel M., Schmutz W. & Sokal, K.R. 2010, *AJ*, 139, 825
- van der Hucht, K.A. 2001, *New Astronomy Rev.*, 45, 135
- van der Hucht, K.A., Cassinelli, J.P., & Williams P.M. 1986, *A&A*, 168, 111
- Vuong, M.H., Montmerle, T., Grosso, N., Geigelson, E.D., Verstraete, L., & Ozawa, H. 2005, *A&A*, 408, 581
- White, R.L. & Becker, R.H. 1995, *ApJ*, 451, 352
- Williams, P.M. 1995, ‘Wolf-Rayet Stars: binaries, colliding winds, evolution’, *Proceedings IAU Symposium no. 163*, eds. K.A. van der Hucht and P.M.Williams, Kluwer Academic Publishers, Dordrecht, 335
- Williams, P.M. 2008, *Revista Mexicana AA (Serie de Conferencias)*, 33, 71



- Williams, P.M. 2011, Socit Royale des Sciences de Lige, Bulletin, 80, 595
- Williams, P.M., Kidger, M.R., van der Hucht, K.A. et al. 2001, MNRAS, 324, 156
- Williams, P.M., van der Hucht, K.A., Pollock, A.M.T., Florkowski, D.R., van der Woerd, H., & Wamsteker, W. 1990, MNRAS, 243, 662
- Williams, P.M., van der Hucht, K.A., van Wyk, F., Marang, F., Whitelock, P.A., Bouchet, B., & Setia Gunawan, D.Y.A.. 2012, MNRAS, 420, 2026
- Zhekov, S.A. 2007, MNRAS, 382, 886
- Zhekov, S.A. 2012, MNRAS, 422, 1322
- Zhekov, S.A., Gagné, M. & Skinner, S.L. 2011, ApJ, 727, L17
- Zhekov, S.A., Gagné, M. & Skinner, S.L. 2014, ApJ, 785, 8
- Zhekov, S.A. & Skinner, S.L. 2000, ApJ, 538, 808
- Zhekov, S.A., Tomov, T., Gawronski, M.P., Georgiev, L.N., Borissova, J., Kurtev, R., Gagné, M. & Hajduk, M. 2014, MNRAS, 445, 1663

This paper has been typeset from a  $\text{\LaTeX}$  file prepared by the author.